

Transport Effects on Signal Propagation in Quantum Wires

Sayeeff Salahuddin, Mark Lundstrom, *Fellow, IEEE*, and Supriyo Datta, *Fellow, IEEE*

Abstract—Currently, nanowire-based circuits are being considered as candidates for future high-speed electronics. Signal propagation in metallic carbon nanotubes has been analyzed using the Luttinger liquid theory to develop a transmission-line model showing features that can not be obtained from a conventional transmission-line theory. The Luttinger liquid theory, however, is governed by strict conditions which restrict its application to metallic carbon nanotubes and it can not be used for any nanowire in general. In this paper, we present a unified theory that can be applied to wires ranging all the way from conventional three-dimensional conductors to one-dimensional carbon nanotubes. We show that when the number of current-carrying modes is less than a critical value, and the small-signal propagation characteristics are significantly influenced by transport effects which go beyond the conventional transmission-line theory. We also use our model to quantitatively examine a few potential applications.

Index Terms—Boltzmann transport equation (BTE), interconnect, kinetic inductance, nanowires, quantum capacitance, transmission-line.

I. INTRODUCTION

INTERCONNECTS for integrated circuits have traditionally been fabricated out of metals like copper and aluminum. However, with the continued downscaling of the cross section, alternative possibilities are being considered. Perhaps the most well-known are metallic carbon nanotubes for which a novel transmission-line model has been proposed based on Luttinger liquid theory [1]–[10] which was applied by Burke [11], [12] to evaluate potential applications. Recently, a performance comparison between metallic CNTs and Cu wires was done regarding their interconnect applications based on Burkes study [13]. This pioneering work of Burke in introducing Luttinger liquid-based transmission-line models to the engineering literature raises an interesting question. While a traditional interconnect (see Fig. 1) is modeled as a transmission-line having a magnetic inductance, L_M and an electrostatic capacitance, C_E (see Fig. 2), the Luttinger liquid based model has an additional kinetic inductance L_K and a quantum capacitance, C_Q (see Fig. 3). What is the relation between these extremes? Would a copper wire have the additional inductance/capacitance if its cross section were reduced sufficiently? If so, how much?

Manuscript received January 28, 2005; revised May 3, 2005. This work was supported by the MARCO focus center for Materials, Structure and Devices, and by the National Science Foundation. The review of this paper was arranged by Editor R. Singh.

The authors are with the School of Electrical and Computer Engineering, Purdue University, West Lafayette, IN 47906 USA.

Digital Object Identifier 10.1109/TED.2005.852170

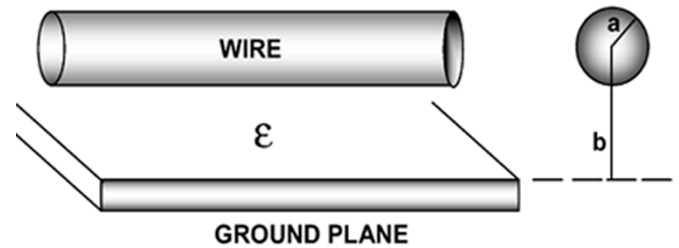


Fig. 1. Wire and the ground plane geometry. The radius of the wire is a , and b is the distance from ground plane. The material between wire and ground plane has a dielectric permittivity of ϵ_r .

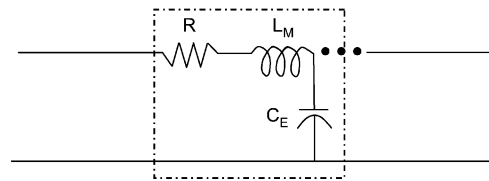


Fig. 2. Conventional transmission-line. The resistance and the inductance are in series. The resistance results from the finite conductivity of the transmission-line. The shunt line consists of a capacitance between the wire and the ground plane. For simplicity, we have ignored the shunt conductance which results from the lossy properties of the intermediate dielectric.

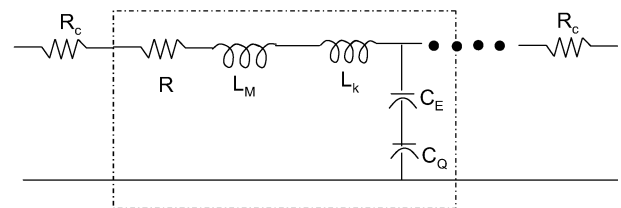


Fig. 3. Proposed equivalent circuit of a long wire. The total inductance is a series combination of magnetic and kinetic inductance. The total capacitance is a series combination of electrostatic and quantum capacitance.

In this paper, we try to provide a compact answer to this question. We show that for an arbitrary nanowire having a set of transverse modes or subbands with dispersion relations $E_m(k)$ (not necessarily parabolic, see Fig. 4), the additional inductance and capacitance are given by

$$C_Q = G_0 \sum_m \overline{(1/v_m)} \quad (1)$$

$$1/L_k = G_0 \sum_m \overline{v_m} \quad (2)$$

where G_0 is the conductance quantum ($= 2e^2/h$) and $\overline{v_m}$ is the thermally averaged velocity of electrons in mode “ m .” This

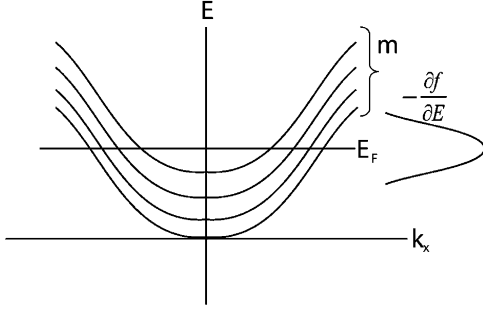


Fig. 4. Typical E - k diagram of a semiconductor showing relative position of conduction band edge, Fermi level E_F , and subbands. The Lorentzian shape of the derivative of the distribution function is also shown.

is the central result which we derive from a semiclassical transport theory (based on the Boltzmann equation) without invoking any new concepts like Luttinger liquids¹. The derivation also helps bring out an important conceptual issue, namely that the “voltage” in the transmission-line model represents the quasi-Fermi level and not the electrostatic potential.

If we specialize to a metallic nanotube with two subbands having linear dispersion relations $E_m(k) = \hbar v_F k$, (1) and (2) yield the Luttinger liquid results

$$C_Q = G_0/v_F \quad \text{and} \quad 1/L_K = G_0 v_F. \quad (3)$$

However, the real value of (1) and (2) is that they allow us to evaluate C_Q and L_K for arbitrary nanowires including copper interconnects with small cross sections. Indeed, we could write approximately

$$C_Q \sim M G_0 / \langle v \rangle \quad \text{and} \quad 1/L_K \sim M G_0 \langle v \rangle \quad (4)$$

where $\langle v \rangle$ is an average velocity and M is the total number of modes or subbands. For those who are more familiar with DOS (per unit length), D , we note that the number of modes M is $\sim D/\hbar \langle v \rangle$, but it is more convenient to state our results in terms of modes. The number of modes M is roughly equal to the number of half-wavelengths (electronic) that fit into the cross section (just like the modes of an electromagnetic waveguide) and increases linearly with the cross-sectional area S .

It is easy to see from (4) why we do not worry about C_Q and L_K in wires with large cross sections S . Once M is large enough, $C_Q \gg C_E$ and $L_K \ll L_M$ and can be ignored, taking us back to the standard transmission-line model with just L_M and C_E . What value of M is large enough? If we require that the quantum capacitance exceeds $2\pi\epsilon$ (neglecting the geometry specific factors) we get from (4)

$$M > (\epsilon_r)(\pi/2) \times 137 \times (\langle v \rangle / c) \sim \epsilon_r \quad (5)$$

showing that a wire with tens of modes will have a C_Q large enough that it can be neglected. Interestingly, it takes a far larger value of M to make the kinetic inductance small enough to be neglected. This can be seen by noting that $L_M C_E = 1/c^2$, c

¹Note that the Luttinger Liquid theory is needed to calculate the modification of single electron properties like density of states (DOS) due to strong electron-electron correlation which we do not address in this paper.

being the velocity of light, while from (4), we can write $L_K C_Q = 1/\langle v \rangle^2$. Hence

$$(L_M/L_K)(C_E/C_Q) = (v/c)^2 \sim 10^{-4}. \quad (6)$$

This means that in order for L_M/L_K to be less than 1, C_Q/C_E needs to exceed 10^4 , thus requiring the number of modes to exceed several thousands. For copper wires, this would require a cross section of at least 10×10 nm, assuming the electron wavelength to be 0.2 nm.

There is, however, another way one could evaluate the importance of retaining L_K : by comparing its impedance to the series resistance rather than to the magnetic inductance L_M . The usual series resistance can also be expressed in a form similar to (1) and (2)

$$1/R = G_0 \sum_m \bar{v}_m \tau \quad (7)$$

τ being the momentum relaxation time. This means that for ωL_K to exceed R , the frequency ω must exceed $1/\tau$. Since τ is typically $\sim 10^{-12}$ s, this means that for frequencies less than a terahertz, the kinetic inductance is overwhelmed by the series resistance. This is why the kinetic inductance acquires a greater significance in ballistic conductors for which τ is effectively infinite. Thus, there are two independent factors that can make the kinetic inductance significant in nanowires: A long τ is needed to make L_K exceed R/ω for relatively low frequencies, while a small M is needed to make L_K exceed L_M .

Finally, we note that we can associate each mode m with its own individual transmission-line having a kinetic inductance and a quantum capacitance given by (1) and (2), but without the summation over m . The electrostatic capacitance then appears as a self/mutual capacitance connecting the individual transmission-lines. For metallic carbon nanotubes with four modes, two associated with each spin, Burke [11] showed that such a model predicts the correct spin wave velocities in addition to the charge wave velocity. In this paper, however, we restrict ourselves to the charge mode alone assuming that all the transmission-lines representing the individual modes operate in phase so that the associated inductances and capacitances can all be added as shown in (1) and (2).

Let us now proceed to derive our central results, namely (1) and (2) and apply them to a few illustrative examples (Section IV).

II. DERIVATION OF TRANSMISSION LINE EQUATIONS

A. Transport Equations From BTE

The Boltzmann transport equation (BTE) is written as

$$\frac{\partial f}{\partial t} + \vec{v} \cdot \vec{\nabla} f - \frac{e}{\hbar} \vec{\xi} \cdot \vec{\nabla}_k f = S_{\text{op}} f. \quad (8)$$

Let us assume that there is a time-dependent electric field only in the x direction which is also the transport direction. We also assume confinement in the y and z directions. Then in (8) we can use $\vec{v} \equiv v \hat{x}$ and $\vec{k} \equiv k \hat{x}$. We now write the distribution function in (8) as $f(m, k, x, t) = 1/(1 + e^{E(m, k, x, t)/k_B T})$, m being the index of subbands that arise due to the confinement in y and z

directions (see Fig. 4). Assuming local equilibrium, the energy variable E is written as

$$E = \epsilon_m(k) + U(x, t) - \mu(x, t) \quad (9)$$

where μ is the electrochemical and U is the electrostatic potential energy. We can now rewrite (8)

$$\frac{\partial f}{\partial t} + v \frac{\partial f}{\partial x} - \frac{e}{\hbar} \xi \frac{\partial f}{\partial k} = S_{\text{op}} f. \quad (10)$$

As shown in Appendix A, (10) can be written as

$$\frac{\partial f}{\partial t} + v \left(-\frac{\partial f_0}{\partial E} \right) \frac{\partial \mu}{\partial x} = S_{\text{op}} f \quad (11)$$

where $f_0(E)$ is the equilibrium Fermi function. Now multiplying (11) by $(-ev/L)$ and summing over (m, k) one may obtain²³

$$\frac{\partial I}{\partial t} + \frac{I}{\tau} = -\frac{1}{L_k} \frac{\partial(-\mu/e)}{\partial x}. \quad (12)$$

In this equation

$$1/L_k = \frac{e^2}{L} \sum_{m,k} v^2 \left(-\frac{\partial f_0}{\partial E} \right) \quad (13)$$

L being the length of the wire.

Next, we consider the quantum capacitance. We start by writing the charge density per unit length as $\rho = -e \sum_{m,k} f$. Then, the total quantum capacitance $(d\rho/d\mu)$ per unit length [14] is given by

$$C_Q = \frac{e^2}{L} \sum_{m,k} \left(-\frac{\partial f_0}{\partial E} \right) = e^2 \bar{D}_0 \quad (14)$$

where \bar{D}_0 is the temperature averaged DOS per unit length, i.e., the average DOS around the Fermi level per unit length and has the following expression

$$\bar{D}_0 = \int dE D(E) \left(-\frac{\partial f_0}{\partial E} \right). \quad (15)$$

Note that the expression for C_Q in (14) may be also written as

$$\begin{aligned} C_Q &= \frac{e^2}{L} \sum_{m,k} \left(-\frac{\partial f_0}{\partial E} \right) \\ &= e^2 \sum_m \int \frac{dE}{\pi \hbar v_m(E)} \left(-\frac{\partial f_0}{\partial E} \right) \\ &= \frac{e^2}{\pi \hbar} \sum_m \overline{(1/v_m)} \end{aligned}$$

which gives us (1). In the same way (13) can be manipulated to yield (2). Now from (13) and (14) one may obtain

$$\begin{aligned} \frac{1}{L_k C_Q} &= \frac{e^2 \sum_{m,k} v^2 \left(-\frac{\partial f_0}{\partial E} \right)}{e^2 \sum_{m,k} \left(-\frac{\partial f_0}{\partial E} \right)} \\ &= \langle v^2 \rangle. \end{aligned} \quad (16)$$

Physically $\langle v^2 \rangle$ is the average of the square of velocity components for each subband over the energy range spanned by the derivative of the distribution function (see Fig. 4). Note that this way of averaging is a little different from usual in the sense that we are using the derivative of the distribution function with respect to energy $(-\partial f_0/\partial E)$ rather than the distribution function f itself as the weighting factor. This difference arises because we are only interested in the *variations* in different quantities due to a small time-dependent signal. Following (16), in this paper, we shall define the average of any quantity ϑ as

$$\langle \vartheta \rangle = \frac{e^2 \sum_{m,k} \vartheta \left(-\frac{\partial f_0}{\partial E} \right)}{e^2 \sum_{m,k} \left(-\frac{\partial f_0}{\partial E} \right)}. \quad (17)$$

Equation (12) gives us one transmission-line equation. The second one is obtained by combining current continuity equation $(\partial \rho/\partial t) = -(\partial I/\partial x)^4$ with $C_E(-U/e) = \rho^5$, where C_E is the electrostatic capacitance per unit length computed using the Poissons equation subjected to proper boundary conditions [15], and ρ is the charge per unit length. We then have

$$C_E \frac{\partial \psi}{\partial t} = -\frac{\partial I}{\partial x}, \quad (18)$$

where following the usual convention, we have defined the electrostatic potential as $\psi = -U/e$.

B. Electrochemical and Electrostatic Potential

We have two choices for the potential: 1) electrochemical potential [see (12)] and 2) electrostatic potential [see (18)]. We need to express both equations in terms of one or the other. A volt meter will measure the electrochemical and not the electrostatic potential and so we choose the former. We also find that this choice leads to more physically transparent model parameters. Now the problem is to relate the electrochemical potential to the electrostatic potential. Let us assume that a packet of charge density $(-e\delta n)$ is moving in the positive x direction. When it reaches a specific point inside the wire, the bottom of the conduction band moves up by an amount $\Delta E_c = (e^2 \delta n / C_E) = \delta U$ due to electrostatic energy (see Fig. 5). The Fermi level has to move up, too, to make space for the extra electron density δn . How much the Fermi level moves up is determined by the DOS. Let us assume that for the specific system under consideration, the Fermi level moves up by an amount of $\Delta \mu = \delta \mu$ from its equilibrium position μ_0 . Then, from $n = \int dE D(E) f(E)$ and using (9) we obtain

$$\begin{aligned} \delta n &= \frac{\partial n}{\partial E} (\delta U - \delta \mu) \\ e^2 \delta n &= -e^2 \frac{\partial n}{\partial E} (\delta \mu - \delta U) = C_E \delta U. \end{aligned} \quad (19)$$

⁴One may obtain the continuity equation by taking the zeroth moment of the BTE.

⁵This is same as $Q = C_E V$ where, Q is the electrostatic charge and V is the electrostatic voltage.

²This is equivalent to taking the first moment of the BTE.

³In this analysis, τ is defined as $\sum_{m,k} S_{\text{op}} f(-ev/L) = I/\tau$.

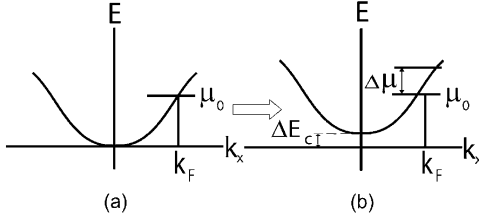


Fig. 5. Both the bottom of the conduction band and Fermi level float up to account for the extra charge δn . The change in the conduction band determines electrostatic potential and the change in Fermi level determines electrochemical potential.

From (14) one may recognize that $-e^2(\partial n/\partial E) = C_Q$. Then, from (19) we obtain

$$\begin{aligned} C_Q(\delta\mu - \delta U) &= C_E\delta U \\ C_E\delta U &= C\delta\mu. \end{aligned} \quad (20)$$

Here, C is defined as

$$C = \frac{C_EC_Q}{C_E + C_Q} \quad (21)$$

which means that C is a series combination of electrostatic and quantum capacitances.

C. Transmission Line Equations

Substituting (20) in (18) and rewriting (12) we have ($\phi_n \equiv -\mu/e$)

$$L_k \frac{\partial I}{\partial t} + RI = -\frac{\partial \phi_n}{\partial x} \quad (22)$$

$$C \frac{\partial \phi_n}{\partial t} = -\frac{\partial I}{\partial x}. \quad (23)$$

Here, we have defined the resistance per unit length as

$$R = L_k/\tau. \quad (24)$$

From (2) and (24) one may obtain (7).

Equations (22) and (23) constitute the lossy-transmission-line equations. All the transmission-line parameters e.g., R , L_k , and C are in the units of per unit length and were obtained in Sections II-A–C. The results stated earlier ((1), (2), (24)) can be expressed in terms of the number of current carrying modes \bar{M} in a conductor, which is defined by the following expression (see Appendix B):

$$\bar{M} = \frac{\pi}{2L} \sum_{m,k} \hbar |v| \left(-\frac{\partial f_0}{\partial E} \right) = \langle |v| \rangle \bar{D}_0 \quad (25)$$

where v is defined as $v = (1/\hbar)(\partial E/\partial k)$. Note that \bar{M} is not quite the number of modes in its true sense, rather, it is the average number of modes around the Fermi level. Using the expression for \bar{M} one can obtain the following expressions for C_Q , L_k , and R :

$$C_Q = \frac{2\bar{M}G_0}{\langle |v| \rangle} \quad (26)$$

$$\frac{1}{L_k} = \frac{2\bar{M}G_0}{\langle |v| \rangle} \langle v^2 \rangle \quad (27)$$

$$R = \frac{1}{G_0 \bar{M} \lambda}. \quad (28)$$

Comparing (28) with (24) and using (2) one may define the mean-free path for backscattering as

$$\lambda = \sum_m 2v_m \tau. \quad (29)$$

D. Magnetic Inductance

In deriving (22), we have not considered the magnetic inductance. If BTE is solved together with Maxwell's equations there will be an additional inductance which has its origin in the magnetic field distribution of the system. A mathematical derivation is provided in Appendix C). However, the end result is fairly intuitive namely, that the magnetic inductance L_M is in series with the kinetic inductance L_k as shown in Fig. 3. Including L_M we can rewrite (22) and (23) as

$$(L_k + L_M) \frac{\partial I}{\partial t} + RI = -\frac{\partial \phi_n}{\partial x} \quad (30)$$

$$C \frac{\partial \phi_n}{\partial t} = -\frac{\partial I}{\partial x} \quad (31)$$

which constitute the transmission-line equations.

E. Contact Resistance

Note that a lumped resistor has to be added to each end (Fig. 3) which originates from the contact resistance given by $1/G_0$ [16]. Typically for a long wire the contact resistance is not important as the dynamic behavior is dominated by the wire itself, but for small systems one can not ignore its effects. In this analysis we shall assume that the contacts are symmetric such that the contact resistance can be equally divided between them so that $R_c = 1/2G_0$. We note here that we have ignored the skin effect in our model. However, with ongoing miniaturization, the cross-sectional area of the wires is becoming increasingly small making the skin effect less and less effective. Therefore, ignoring the skin effect may be deemed as a valid assumption.

III. WAVE VELOCITY

The wave velocity of the transmission-line can be written as

$$v_s^2 = \frac{1}{LC}. \quad (32)$$

A. Conventional Wires

Let us first consider a conventional wire with large cross-section, for which the number of current carrying modes \bar{M} is very high. As a result the kinetic inductance $L_k \propto (1/\bar{M}) \ll L_M$ and the quantum capacitance $C_Q \propto \bar{M} \gg C_E$. This means that the total inductance is $L = L_k + L_M \approx L_M$ and the total capacitance is $C = (C_EC_Q)/(C_E + C_Q) \approx C_E$. Then in the lossless limit, the wave velocity will be given by

$$v_s^2 = \frac{1}{LC} \approx \frac{1}{L_M C_E}. \quad (33)$$

This is, of course, what is predicted from conventional transmission-line theory.

B. Nanowires: Metallic Carbon Nanotubes

Now let us examine a nanowire, specifically a metallic carbon nanotube. Since the DOS is relatively small, we need to care-

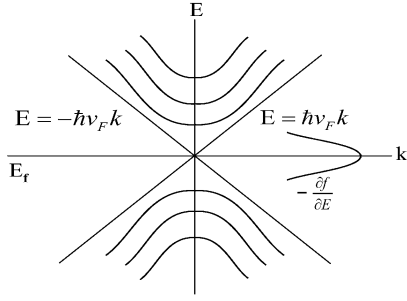


Fig. 6. Schematic E-k diagram of a metallic CNT for one valley. The dispersion relation for the lowest band is given by $E = \pm\hbar v_F k$.

fully consider for the relative values of different components of inductance and capacitance. The magnitude of magnetic inductance depends on geometry, but as a simple estimate one can say that the magnitude will be on the order of $\mu/2\pi \sim 10^{-4}$ nH/ μm . Fig. 6 shows the $E - k$ relationship of a metallic CNT for one valley. For small diameter nanotubes, only the lowest subband with $E = \pm\hbar v_F k$ contributes, so that $\bar{M} = 2$ (due to two valleys) and $v_x = v_F$, $\langle v_x^2 \rangle = \langle v_x \rangle^2 = v_F^2$, and $L_k = 1/4G_0 v_F \approx 1$ nH/ μm . This means that $L_k \gg L_M$. Hence, the total inductance is $L = L_M + L_k \approx L_k$. Then in the loss-less limit we may find the wave velocity from

$$\begin{aligned} v_s^2 &= \frac{1}{LC} = \frac{1}{L_k C} = v_F^2 + 4\bar{M} v_F \frac{e^2}{h C_E} \quad \text{i.e.,} \\ v_s^2 &= v_F^2 + 8v_F v_0, \end{aligned} \quad (34)$$

where v_0 is defined as $v_0 = e^2/(h C_E)$. This result for wave velocity exactly matches the result predicted from Luttinger liquid theory [17].

C. Critical Number of Modes

From the above analysis of metallic CNT, it is evident that one can not use conventional methods for evaluating nanowires. We can do a simple calculation to estimate how many modes are required so that kinetic inductance and quantum capacitance can be ignored and conventional transmission-line theory can be applied without modification. Let us first look at the ratio of quantum capacitance and electrostatic capacitance. Using the expression for C_Q from (26) one can show that

$$\frac{C_Q}{C_E} \approx \alpha \left(\frac{c}{\langle |v| \rangle} \right) \left(\frac{4\bar{M}}{\pi \epsilon_r} \right) \quad (35)$$

$\alpha = e^2/4\pi\epsilon_0\hbar c = 1/137$ being the well-known fine structure constant.

Writing the magnetic inductance as $L_M = \epsilon_r/(c^2 C_E)$ we may similarly obtain the ratio of magnetic and kinetic inductances as

$$\begin{aligned} \frac{L_M}{L_k} &= \alpha \left(\frac{c}{\langle |v| \rangle} \right) \left(\frac{4\bar{M}}{\pi} \right) \left(\frac{\langle v^2 \rangle}{c^2} \right) \\ &= \frac{C_Q \epsilon_r \langle v^2 \rangle}{C_E c^2}. \end{aligned} \quad (36)$$

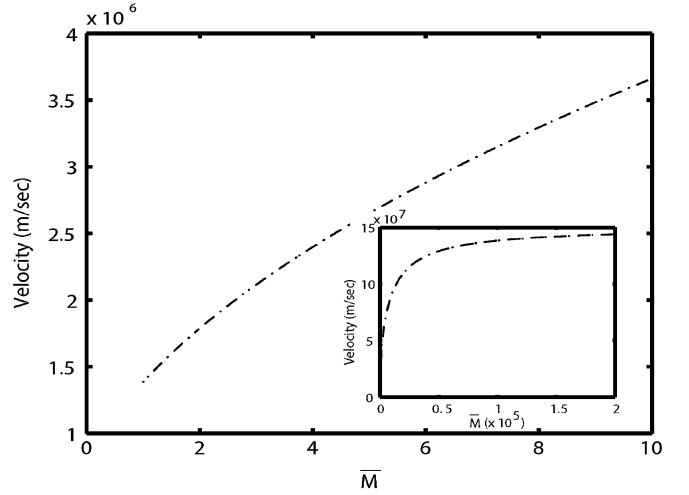


Fig. 7. Variation of wave velocity with DOS. The wave velocity increases with increasing DOS. The inset shows that the velocity saturates at a velocity given by $1/(\sqrt{L_M C_E})$.

It is clear that if $L_M/L_k \gg 1$, C_Q/C_E will also be much larger than 1, since $\epsilon_r \langle v^2 \rangle / c^2$ is typically a small number $\sim 10^{-3}$. This means that the minimum number of modes \bar{M}_c needed for conventional theory to be valid is obtained by requiring $L_M/L_k \gg 1$

$$\bar{M} \gg \frac{\pi \langle |v| \rangle c}{4\alpha \langle v^2 \rangle} \equiv M_c \sim 10^4. \quad (37)$$

To illustrate this effect numerically we plot the variation of wave velocity v_s with number of modes \bar{M} in Fig. 7 for $\epsilon_r = 4$. The plot shows that the wave velocity increases with number of modes. The inset shows that for high enough \bar{M} , the wave velocity saturates to a value given by $c/\sqrt{\epsilon_r}$. This agrees with the two limiting examples that we have considered and our model allows one to bridge across these limits in a consistent manner.

IV. APPLICATION

In this section we shall use the aforementioned method to explore a few potential applications of nanowires including; a) nanowires as interconnects, b) a comparison of metallic CNT and the Cu interconnects and, c) nanowires as nanoresonators.

A. Nanowires as Interconnects

We shall take the metallic CNT as a specific example. For simplicity, we shall assume that the wire and the nearby ground plane can be described by a coaxial geometry, so that the electrostatic capacitance per unit length is $2\pi\epsilon/\ln(b/a)$ and the magnetic inductance per unit length is $(\mu/2\pi) \ln(b/a)$, where a and b are the radius of the wire and distance from the ground plane respectively (see Fig. 1). We shall assume $b/a = 10$. In addition, for a metallic CNT $v_F = 8 \times 10^5$ m/s. Table I shows the resulting transmission-line parameters for a metallic CNT. From this specific example, we see that the kinetic inductance is indeed 10 000 times larger than the magnetic inductance. Using the values shown in Table I, the wave velocity is found to be $v_s = 1.78 \times 10^6$ m/s.

TABLE I
TRANSMISSION-LINE PARAMETERS OF A METALLIC CNT FOR A GIVEN GEOMETRY. FOR SPECIFIC VALUES OF THE GEOMETRICAL PARAMETERS PLEASE REFER THE TEXT

$Z_C/2$	C_E	C_Q	L_M	L_k
(k Ω)	(aF/ μ m)	(aF/ μ m)	(nH/ μ m)	(nH/ μ m)
3.2393	97	386	4.6×10^{-4}	4.05

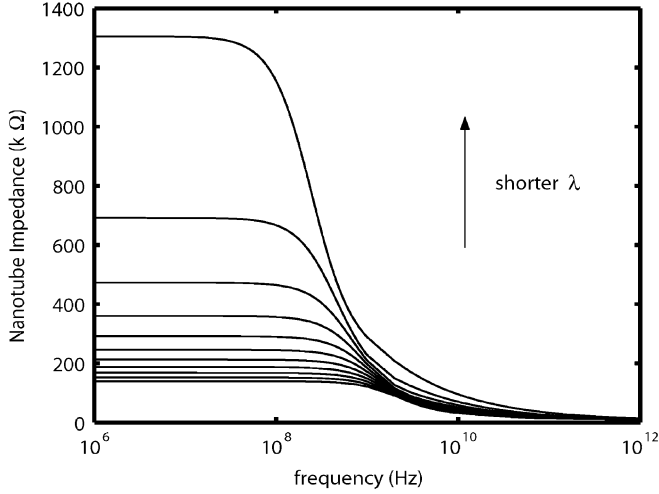


Fig. 8. Variation of dynamic impedance of a metallic CNT with frequency for different scattering lengths. The length of the wire is 100 μ m.

Fig. 8 shows the dynamic impedance of a 100- μ m-long metallic carbon nanotube for different scattering lengths. The dynamic impedance is calculated as

$$Z_{\text{dynamic}} = R_C + Z_0 \frac{1 + \rho e^{-2\gamma l}}{1 - \rho e^{2\gamma l}} \quad (38)$$

where $Z = R + j\omega L$, $Y = j\omega C$, $Z_0 = \sqrt{Z/Y}$, $\gamma = \sqrt{YZ}$, $\rho = (Z_L - Z_0)/(Z_L + Z_0)$, and $Z_L = R_C$. The scattering mean-free path is varied over a range of 0.5–5 μ m. The frequencies of interest are the points where the impedance shows a sharp change. The first point is determined by $\omega = 1/RC$ and the second one by $\omega = R/L$. From the figure, for a 100 μ m wire, the first one varies from 0.5–5 GHz and the second one varies from 10–50 GHz. Therefore, in a long enough metallic nanotube, these frequencies should be experimentally measurable. At low frequency, however, the latency of the wire is dominated by the RC time constant. The resistance of the metallic CNT, typically a few k Ω s, is much greater than that of a conventional interconnect. This high resistance will make the metallic CNT slower compared to the conventional interconnects. When the frequency is high and the latency is determined by L and C , metallic nanotube is still slower due to its huge kinetic inductance.

The above analysis is, in general, applicable to all types of nanowires. The confinement of electrons for a 1-D system severely decreases the number of propagating modes. This results in increased resistance and kinetic inductance. Therefore, one can say that in general a single nanowire will be slow as an interconnect.

B. Comparison of Metallic CNTs With Cu Interconnects

One way to increase the speed of the nanowires is to increase the number of modes or the number of subbands. Geometrically, the number of subbands is limited by the diameter and band structure of the specific nanowire. For a given dimension for the nanowire, it may be worthwhile to examine how a parallel combination of many nanowires, occupying the same amount of space as conventional interconnects, compare with them in performance. For a specific example, let us again choose the metallic carbon nanotube. For simplicity, we shall assume that when we put the metallic CNTs in parallel, they are noninteracting in nature. In this limit, paralleling simply means adding degenerate subbands. The DOS of this total parallel system will be the DOS for a single CNT times the number of wires in parallel.

As for the structure, we assume a height of 100 nm and a width of 50 nm. The resistivity and inductance for a Cu interconnect with these dimensions is predicted to be about 9.5 k Ω /mm and 2 nH/mm, respectively, [18]. This means that if we have approximately 1000 nanotubes in parallel, the inductance will be similar to that of a copper wire. If we consider nanotubes of a diameter of 2 nm, the cross section is big enough to hold $150 \times 100/\pi \approx 5000$ nanotubes. Therefore, for high frequency, where wave velocity is determined by L and C , if enough CNTs can be put in parallel, the speed will be only constrained by the fundamental limit of $c/\sqrt{\epsilon_r}$. At low frequency, however, the RC time constant dominates and we need to figure out individual resistivities of Cu and CNT for a comparison of latency.

Let us consider the Cu interconnect first. At $T = 0$ K, \bar{M} can be estimated from (25) as $\bar{M} = S(h/4)v_F D(E_F)$, $D(E_F)$ being the total DOS per unit volume at the Fermi energy and S , the cross-sectional area. We shall use the known values of v_F and $D(E_F)$ for Cu from [19]. From this one can obtain the variation of resistance with length from

$$R = (h/2e^2 \bar{M})(1 + l/\lambda). \quad (39)$$

However, one needs to worry about what λ to use in this equation. The mean-free path depends on different scattering mechanisms, which in turn depends on specific structure and geometry. While there is continuing research to find out appropriate λ , for first order estimate, we shall base our calculations on the results predicted by [18]. As was mentioned earlier, for the geometry under consideration the predicted resistivity is about 9.5 k Ω /mm. Using this value in (39), we estimate $\lambda \approx 15.6$ nm which is significantly smaller than the bulk value of 39.3 nm [20].

For metallic CNTs, at the low field, only acoustic phonons are effective. However, in the high field the optical phonons enter the picture as well. To model these effects we shall follow the same procedure as [21]. For low field transport we shall assume a mean-free path $\lambda_{\text{acc}} = 1.6 \mu$ m as estimated from experimental data. For high field transport electrons require a finite length, L_t , to travel before they acquire the energy (0.16 eV) to emit an optical phonon. Then the total length that the electron travels under optical phonon scattering is $(L_t + L_{\text{hp}})$ where $L_{\text{hp}} \approx 30$

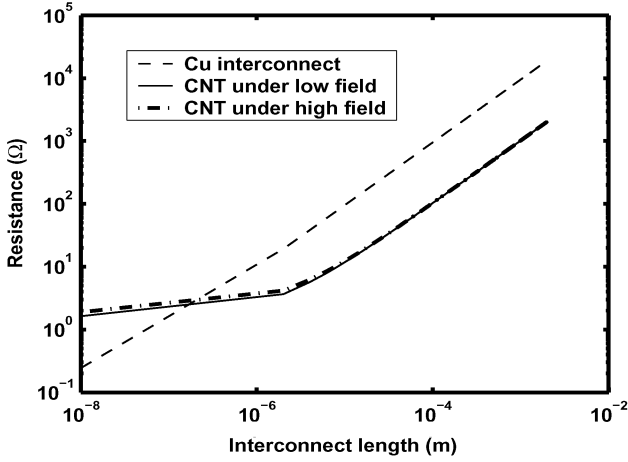


Fig. 9. Comparison of resistance with length for a Cu interconnect and a parallel combination of metallic CNTs.

nm is the optical phonon scattering mean-free path. Then the resistance of a metallic CNT can be modeled as

$$R = \frac{h}{4e^2} \left[1 + \frac{l}{\lambda_{\text{acc}}} \right]; \quad \text{low field}$$

$$= \frac{h}{4e^2} \left[1 + l \left(\frac{1}{\lambda_{\text{acc}}} + \frac{1}{0.16L/V + L_{\text{hp}}} \right) \right]; \quad \text{high field}$$

where L is the length of the wire, V is the applied voltage and $L_t = 0.16L/V$. Fig. 9 shows the variation of resistance for the Cu interconnect and 4000 *noninteracting* metallic CNTs in parallel. We have assumed $V = 0.5$ V for the high field transport.

From Fig. 9, the effect of ballisticity of CNTs is evident. The nanotube resistivity is only affected by the contact resistance up to a significant length. As a result, the upward turn of the resistivity curve occurs much later for a CNT compared to the Cu wire. This is why CNT shows a smaller resistance compared to Cu wires for larger lengths. For very short lengths the resistivity for CNT is higher due to higher contact resistance resulting from smaller number of modes compared to the Cu wire. The bottom line is, if enough CNTs can be put in parallel, the performance may be comparable or better than the Cu wire.

It should be mentioned that we have assumed the CNTs to be noninteracting. In the real world, one needs to carefully study the interactions to see how they affect the DOS. Once the DOS is known, the proposed method can be used to examine signal propagation properties.

Under high field transport conditions metallic nanotubes have shown a current saturation at 20–25 μA [21]. By contrast, Cu interconnects have a maximum current density of 10^6 A/cm² due to electromigration problems⁶. In that regard, the cross section that we have used in this example can deliver 150 μA current. This means that we only need ~ 10 CNTs to match the current carrying capacity of the Cu interconnect. Therefore, in a current driven circuit or where high power transport is needed, CNTs may be preferred over the Cu interconnect.

⁶Electromigration problems do not occur for CNTs until 10^6 A/cm² [22]

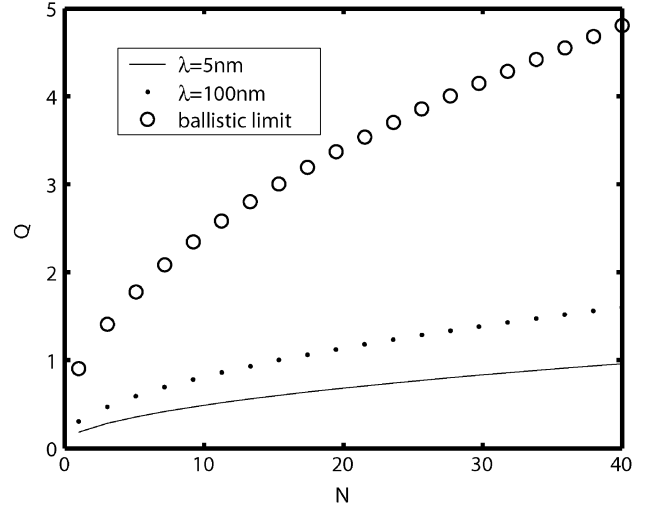


Fig. 10. Variation of Q factor with no. of wires in parallel. For large number of \bar{M} , the Q factor increases approximately as square root of \bar{M} .

C. Nanoresonators

As the nanowires were shown to have a huge kinetic inductance, one possible application of nanowires may be as terahertz oscillators. To examine this possibility we need to know the Q factor. As an example let us consider a metallic CNT. The length of each wire is chosen to be 200 nm. For simplicity we have again assumed a noninteracting case. As indicated in the previous section, for noninteracting system paralleling simply amounts to a direct increase in degenerate subbands, which in turn means an increase in the number of modes \bar{M} . Fig. 10 shows the variation of the Q factor with N where N is the number of wires in parallel. The Q factor shows a monotonic increase with N . This can be understood by noting that in the limit $C_Q > C_E$, the Q factor, given by $Q = 1/R\sqrt{L/C}$ will increase as square root of \bar{M} . It is clear from Fig. 10 that the Q factor is not very impressive. Even for the ballistic case, the Q is just over one for a single CNT. The ability to put CNTs in parallel helps the scenario. However, paralleling also means a decrease in the effective kinetic inductance. This poses an interesting design problem. A reasonable tradeoff may be made to achieve the intended inductance at the required Q .

V. CONCLUSION

In this paper, we have proposed a general model which can be used to examine the wave propagation in any nanowire with a given set of current carrying modes. The proposed method can be used as a common platform to examine and compare wires ranging from conventional 3-D to modern 1-D conductors. We have shown that for quantum wires, electron transport has important influence on the dynamic behavior and needs to be considered carefully. It is predicted that a single quantum wire is inherently slow (see Fig. 7 and 8) and may not prove to be a good interconnect compared to conventional materials. Parallel combinations of many nanowires may prove to be fruitful (see Fig. 9) in this regard and is worth investigating.

APPENDIX

A. Expressing the BTE in Terms of $\partial\mu/\partial x$

From (9) we can write

$$v \frac{\partial f}{\partial x} = v \frac{\partial f_0}{\partial E} \frac{\partial(U - \mu)}{\partial x}, \quad (40)$$

where f_0 is the equilibrium Fermi function. Note that, in (40), by replacing $\partial f/\partial E$ by $\partial f_0/\partial E$ we are ignoring the time-dependence of $\partial f/\partial E$, which is consistent with the so called small signal treatment. In addition, we can write the third term as

$$\begin{aligned} \frac{e}{\hbar} \xi \frac{\partial f}{\partial k} &= \frac{\partial U}{\partial x} \frac{\partial f}{\partial(\hbar k)} \\ &= \frac{\partial U}{\partial x} \frac{\partial f_0}{\partial E} \frac{\partial E}{\partial(\hbar k)} \\ &= v \frac{\partial f_0}{\partial E} \frac{\partial U}{\partial x}. \end{aligned} \quad (41)$$

In writing (41) we have used the relations $\xi = -(\partial(-U/e)/\partial x)$ and $v = (1/\hbar)(\partial E/\partial k)$. Then adding (40) and (41) we have

$$v \frac{\partial f}{\partial x} - \frac{e}{\hbar} \xi \frac{\partial f}{\partial k} = v \left(-\frac{\partial f_0}{\partial E} \right) \frac{\partial \mu}{\partial x}. \quad (42)$$

B. Deriving and Expression for \bar{M}

The current I flowing in a ballistic wire under a small bias can be expressed as

$$I = \frac{2e}{h} \bar{M} d\mu \quad (43)$$

where (43) defines the quantity \bar{M} . We can also write the equation for current as

$$\begin{aligned} I &= \sum_{m,v>0} \frac{e}{L} v \left(-\frac{\partial f_0}{\partial E} \right) d\mu \\ &= \frac{e}{2L} \sum_{m,v} |v| \left(-\frac{\partial f_0}{\partial E} \right) d\mu. \end{aligned} \quad (44)$$

Equating (43) and (44), we have the following expressions for \bar{M} :

$$\bar{M} = \frac{\pi}{2} \sum_{m,k} \hbar |v| \left(-\frac{\partial f_0}{\partial E} \right). \quad (45)$$

C. Coupling Maxwell's Equation to the BTE

In this paper, we have used the Poisson's equation to write the electric field $\xi = \partial(U/e)/\partial x$. If we account for the electromagnetic coupling we can write the electric field as

$$\xi = \frac{\partial(U/e)}{\partial x} - \frac{\partial A}{\partial t} \quad (46)$$

where A is the vector magnetic potential. Using this expression for an electric field, (11) can be written as

$$\frac{\partial f}{\partial t} + v \left(-\frac{\partial f_0}{\partial E} \right) \left(\frac{\partial \mu}{\partial x} + \frac{\partial A}{\partial t} \right) = S_{\text{op}} f. \quad (47)$$

Writing $A = L_M I$ and multiplying both sides of (47) by $\sum_{m,k} (-ev/L)$ one then obtains

$$\begin{aligned} \frac{\partial I}{\partial t} + \frac{1}{L_k} \left(\frac{\partial(-\mu/e)}{\partial x} + L_M \frac{\partial I}{\partial t} \right) &= -\frac{I}{\tau} \\ \left(1 + \frac{L_M}{L_k} \right) \frac{\partial I}{\partial t} + \frac{I}{\tau} &= -\frac{1}{L_k} \frac{\partial(-\mu/e)}{\partial x}. \end{aligned} \quad (48)$$

ACKNOWLEDGMENT

S. Salahuddin would like to thank M. Vaidyanathan, D. Kienle, S. M. Hasan, M. A. Alam, and S. Mohammadi for useful discussions.

REFERENCES

- [1] M. Fisher and L. I. Glazman, "Transport in a one dimensional luttinger liquid," in *Mesoscopic Electron Transport*. Norwell, MA: Kluwer, 1997, pp. 331–373.
- [2] Y. M. Blanter, F. W. J. Hekking, and M. Buttiker, "Interaction constants and dynamic conductance of a gated wire," *Phys. Rev. Lett.*, vol. 81, no. 9, pp. 1925–1928, 1998.
- [3] I. Safi and H. J. Schulz, "Transport in an inhomogeneous interacting one-dimensional system," *Phys. Rev. B*, vol. 52, no. 24, pp. 17 040–17 043, 1995.
- [4] R. Tarkiainen, M. Ahlskog, J. Penttila, L. Roschier, P. Hakonen, M. Paalanen, and E. Sonin, "Multiwalled carbon nanotube: Luttinger versus Fermi liquid," *Phys. Rev. B*, vol. 6419, no. 19, pp. art. no.-195 412–XQXQXQ, 2001.
- [5] V. V. Ponomarenko, "Frequency dependences in transport through a tomonaga-luttinger liquid wire," *Phys. Rev. B*, vol. 54, no. 15, pp. 10 328–10 331, 1996.
- [6] G. Cuniberti, M. Sassetti, and B. Kramer, "Ac conductance of a quantum wire with electron-electron interactions," *Phys. Rev. B*, vol. 57, no. 3, pp. 1515–1526, 1998.
- [7] V. A. Sablikov and B. S. Shchamkhalova, "Dynamic transport of interacting electrons in a mesoscopic quantum wire," *J. Low Temp. Phys.*, vol. 118, no. 5–6, pp. 485–494, 2000.
- [8] Ph.D. dissertation, 1999.
- [9] E. B. Sonin, "Tunneling into 1d and quasi-1d conductors and luttinger-liquid behavior," *J. Low Temp. Phys.*, vol. 124, no. 1–2, pp. 321–334, 2001.
- [10] K. V. Pham, "Interface resistance and ac transport in a luttinger liquid," *Eur. Phys. J. B*, vol. 36, pp. 607–618, 2003.
- [11] P. J. Burke, "Luttinger liquid theory as a model of the gigahertz electrical properties of carbon nanotubes," *IEEE Trans. Nanotechnol.*, vol. 1, no. 3, pp. 129–144, Mar. 2002.
- [12] —, "An rf circuit model for carbon nanotubes," *IEEE Trans. Nanotechnol.*, vol. 2, no. 1, pp. 55–58, Jan. 2003.
- [13] A. Naeemi, R. Savari, and D. Meindl, "Performance comparison between carbon nanotube and copper interconnects for gsi," in *IEDM Tech. Dig.*, 2004, pp. 699–702.
- [14] S. Datta, *Quantum Transport: Atom to Transistor*. Cambridge, MA: Cambridge Univ. Press, 2005.
- [15] S. Ramo and J. Whinnery, *Fields and Waves in Communication Electronics*. New York: Wiley, 2002.
- [16] S. Datta, *Electronic Transport in Mesoscopic Systems*. Cambridge, MA: Cambridge Univ. Press, 1995.
- [17] C. Kane, L. Balents, and M. Fisher, "Coulomb interactions and mesoscopic effects in carbon nanotubes," *Phys. Rev. Lett.*, vol. 79, no. 25, pp. 5086–5089, 1997.

- [18] P. Kapur, J. P. McVittie, and K. C. Saraswat, "Technology and reliability constrained future copper interconnects—Part I: Resistance modeling," *IEEE Trans. Electron Devices*, vol. 49, no. 4, pp. 590–597, Apr. 2002.
- [19] *Handbook of the Band Structure of Elemental Solids*, D. Papacostas, Ed., Plenum, New York, 1986.
- [20] K. Fuchs, "The conductivity of thin metallic films according to the electron theory of metals," in *Proc. Cambridge Philos. Soc.*, vol. 34, 1938.
- [21] J. Y. Park, S. Rosenblatt, Y. Yaish, H. UstUnel, S. Braig, T. A. Arias, P. W. Brouwer, and P. L. McEuen, "Electron-phonon scattering in metallic single-walled carbon nanotubes," *Nano Lett.*, vol. 4, no. 3, pp. 517–520, 2004.
- [22] J. Richardson, "Realistic application of cnts," *Mater. Today*, p. 46, 2004.



Sayeef Salahuddin received the B.Sc. degree in electrical and electronic engineering from the Bangladesh University of Engineering and Technology, Dhaka, Bangladesh, in 2003. He is currently pursuing the Ph.D. degree at the Department of Electronics and Computer Engineering, Purdue University, West Lafayette, IN.

His research interests include design, modeling, simulation, and performance evaluation of exploratory electronic and spintronic devices in the nanometer scale.



Mark Lundstrom (F'94) received the B.E.E. and M.S.E.E. degrees from the University of Minnesota, Minneapolis, in 1973 and 1974, respectively, and the Ph.D. degree from Purdue University, West Lafayette, IN, in 1980.

He is the Scifres Distinguished Professor of Electrical and Computer Engineering at Purdue University, where he also directs the National Science Foundations Network for Computational Nanotechnology. Before attending Purdue, he was with Hewlett-Packard Corporation, Loveland, CO,

working on integrated circuit process development and manufacturing. His current research interests center on the physics of semiconductor devices, especially nanoscale transistors. His previous work includes studies of heterostructure devices, solar cells, heterojunction bipolar transistors, and semiconductor lasers. During the course of his career at Purdue, he has served as Director of the Optoelectronics Research Center and Assistant Dean of the Schools of Engineering.

Dr. Lundstrom is a Fellow of the American Physical Society and the recipient of several awards for teaching and research—most recently a 2005 University Researcher Award from the Semiconductor Industry Corporation for his career contributions to physics and simulation of semiconductor devices.



Supriyo Datta (F'96) was born on February 2, 1954. He received the B.Tech. degree from the Indian Institute of Technology, Kharagpur, in 1975 and the Ph.D. degree from the University of Illinois, Urbana-Champaign, in 1979.

In 1981, he joined Purdue University, West Lafayette, IN, where he is currently the Thomas Duncan Distinguished Professor in the School of Electrical and Computer Engineering. He is the author of *Surface Acoustic Wave Devices* (Englewood Cliffs, NJ: Prentice-Hall, 1986), *Quantum Phenomena* (Reading, MA: Addison-Wesley, 1989), and *Electronic Transport in Mesoscopic Systems* (Cambridge U.K.: Cambridge, 1995). His current research interests are centered around the physics of nanostructures and includes molecular electronics, nanoscale device physics, spin electronics and mesoscopic superconductivity.

Dr. Datta received the NSF Presidential Young Investigator Award and the IEEE Centennial Key to the Future Award in 1984, the Frederick Emmons Terman Award from the ASEE in 1994, and shared the SRC Technical Excellence Award, 2001 and the IEEE Cleo Brunetti Award, 2002 with Mark Lundstrom. He is a Fellow of the American Physical Society (APS) and the Institute of Physics (IOP).